

Compressive sampling strategies for integrated microspectrometers

David J. Brady, Michael E. Gehm, Nikos Pitsianis, and Xiaobai Sun

Duke University, Durham, North Carolina

ABSTRACT

We consider compressive sensing in the context of optical spectroscopy. With compressive sensing, the ratio between the number of measurements and the number of estimated values is less than one, without compromising the fidelity in estimation. A compressive sensing system is composed of a measurement subsystem that maps a signal to digital data and an inference algorithm that maps the data to a signal estimate. The inference algorithm exploits both the information captured in the measurement and certain *a priori* information about the signals of interest, while the measurement subsystem provides complementary, signal-specific information at the lowest sampling rate possible. Codesign of the measurement strategies, the model of *a priori* information, and the inference algorithm is the central problem of system design. This paper describes measurement constraints specific to optical spectrometers, inference models based on physical or statistical characteristics of the signals, as well as linear and nonlinear reconstruction algorithms. We compare the fidelity of sampling and inference strategies over a family of spectral signals.

Keywords: Compressive sensing, spectroscopy, multiplex spectroscopy, adaptive inference

1. INTRODUCTION

Compressive sensing consists of estimation of a signal $\mathbf{s} \in \mathbb{R}^n$ from a measurement $\mathbf{g} \in \mathbb{R}^m$ such that $m < n$. We refer to the mapping $\mathbf{H}|\mathbf{s} \rightarrow \mathbf{g}$ from signal to measurement as “sampling” and the mapping $\mathbf{E}|\mathbf{g} \rightarrow \mathbf{s}_e$ as “inference.” High fidelity inference is possible because signal values are not independent. The challenge of compressive sensing is to codesign \mathbf{H} and \mathbf{E} such that \mathbf{s}_e is a faithful estimate of \mathbf{s} . As we discuss in this paper, various metrics may be considered in comparing \mathbf{s}_e and \mathbf{s} .

Compressive sensing is highly related to matched filter and principal component based measurement, which has a long and well developed history. The history of concepts and strategies for compressive sensing is much too long for a comprehensive survey here. Recent interest is sparked in part by Donoho *et al.*, who measure general functionals of a compressible discretization of a function and recover n values from $O(n^{1/4} \log^{5/2}(n))$ measurements. As a optimization criterion they use the minimization of the 1-norm of the sparse representation of the unknown signal to an orthonormal basis.^{1,2} Rapid progress along these lines by Candés, Baraniuk and others is summarized in publications online at www-dsp.rice.edu/CS/. Compressive sensing work at Duke University originated in group testing strategies for distributed sensor networks and in sensor coding based on reference structure tomography.³ These studies extended to imaging system design under the Compressive Optical Montage Photography Initiative (COMP-I).⁴⁻⁶ Potuluri in his Ph.D. thesis proposes a multiplex optical sensing system for compressive sampling to enable signal reconstruction using fewer measurements.⁷

This paper considers simple strategies for compressive spectroscopy based on linear and quasi-linear inference. Ideally, compression on linear spaces might be based upon direct projection on principal components. Challenges to this strategy in spectroscopy include the nonnegativity of spectral projections, spatial coherence limitations and the difficulty of accurate characterization of spectral statistics. We describe the principles in the co-design of the measurement systems and the inference schemes. In compressive sensing systems, the null space of the measurement mapping is of high dimension. The signal estimate is to be located by the inference integrating *a priori* knowledge about the signals of interest and the measurement. Wilson and Barrett have previously considered an algorithm for separating measurement and null-space components of an object with respect to a given imaging system, where knowledge of the measurement and null spaces is crucial for analyzing the deficiencies of such imaging systems.⁸ We describe in this paper a few particular inference schemes from using *ad hoc* objective functions to their adaptation to signal-specific features.

In Section 2, we describe a spectrometer design for compressive sampling and present a model for spectroscopic measurements. We introduce in Section 3 the inference models and their numerical solutions that were developed for a family of spectral data. We demonstrate signal estimates and evaluate the fidelity of the estimates. Finally we describe in Section 4 the basic codesign principles.

2. SPECTROMETER DESIGN

Compressive spectroscopy makes sense in environments where measurement is expensive or subject to physical limitation. Many spectroscopy applications use CCD focal planes or other large detector arrays on which the cost per measurement is tiny. In the case of diffuse source spectroscopy one may choose in fact to make vastly more measurements than the target number of spectral channels requires.^{9,10} Spectroscopy of very weak sources using photomultiplier arrays or of sources in challenging near or mid-IR spectral ranges using exotic detector materials may provide situations in which compressive measurement is attractive. As an example, we demonstrated in previous work that group testing could be used to minimize the number of InGaAs detector elements needed to characterize narrow band NIR sources.¹¹

While in many cases weak sources are also diffuse, the simplest model for a compressive spectrometer is based on the slit design sketched in Fig. 1. The spectral source is assumed to uniformly illuminate the slit of the spectrometer. If the spectral source is a point source, a combination of cylindrical lenses may be used to expand the source to fully illuminate the slit normal to the plane of the figure while keeping the source focused in the plane of the figure.

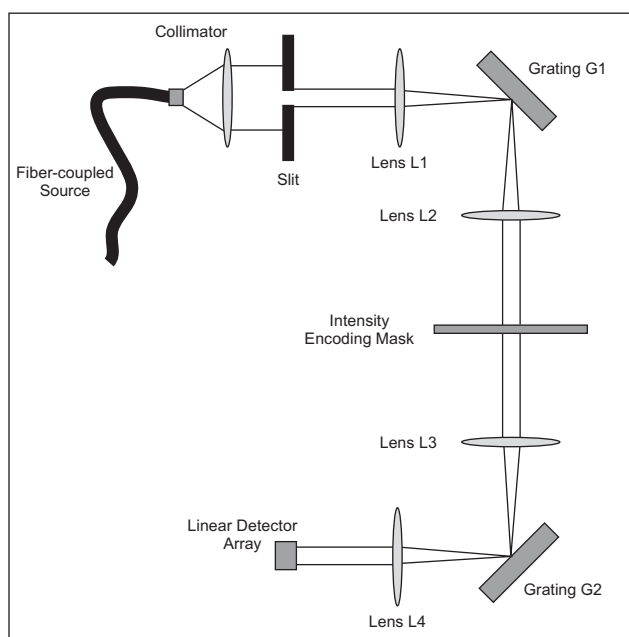


Figure 1. Spectrometer design for compressive sampling.

Another method would be to couple the unknown source into the spectrometer through a fiber. The fiber output is collimated and strikes the input vertical slit. The light from the slit passes through lens L1, is diffracted by grating G1 and then passes through lens L2 before striking the intensity coded mask pattern. The lenses are arranged in a 4-f configuration such that the slit is imaged on to the mask through the grating. The grating causes the image of the slit to vary in horizontal position based on the spectral information in the source. The mask is divided into m rows and N columns, if there are N unknown channels and m sensors. Each element in a row is a filter component, modulating the wavelength corresponding to the corresponding column. The modulation is typically by absorption, meaning that the filter weights are all positive. Negative or complex filter weights

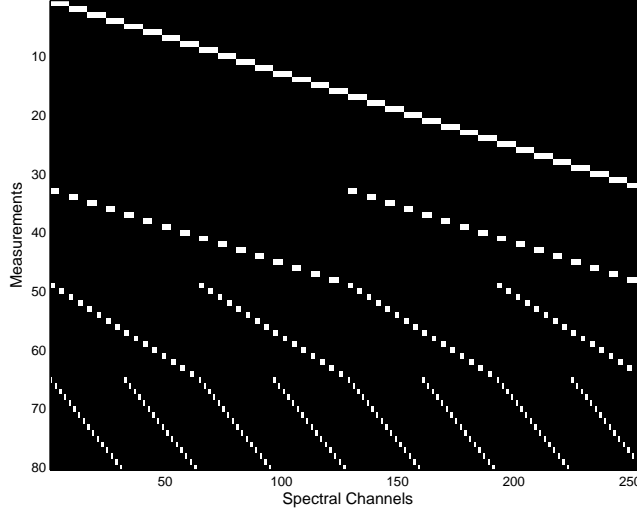


Figure 2. Layout of a correlated mask to implement 31.25% compression. Transmissive and opaque regions are in white and black, respectively.

may be obtained by linear weighting of the output filtered signals. As an example, Fig. 2 shows a compressive sampling mask used in Potuluri’s experiments.⁷

The intensity encoded light then passes through lens L3, strikes grating G2 (which undoes the dispersion introduced by G1) and passes through lens L4 before striking a linear array of photo-detectors. Again, the lenses are arranged in a 4-f configuration, producing an image of the intensity encoded slit on the array of photo-detectors. Thus, when slit is re-imaged through the complementary grating onto an output detector array, each element on the detector array consists of a filtered projection of the input spectrum. Since the filter function corresponds exactly to the transmittance of the mask, any filtering operation may be implemented by this system.

We may represent the transmittance of the coding mask as follows,

$$h(x, y) = \sum_{ij} h_{ij} \text{rect} \left(\frac{x - j\Delta}{\Delta} \right) \text{rect} \left(\frac{y - i\Delta}{\Delta} \right) \quad (1)$$

where $h_{ij} \in \{0, 1\}$. The signal mapped onto on the detector array, for the system of Fig. 1, is $g(y) = \int \int h(x = \lambda, y) s(\lambda) d\lambda$. This signal is integrated over the finite range of the detector elements to obtain

$$g_i = \sum_j h_{ij} s_j \quad (2)$$

where

$$s_j = \int s(\lambda) \text{rect} \left(\frac{\lambda - j\Delta}{\Delta} \right) d\lambda \quad (3)$$

Δ is the width of mask coding elements and Δ_p is the width of the detector pixel. For the rest of the paper a “spectrum” is represented by the vector \mathbf{s} of discrete values s_j , the mapping between the spectrum and the measurements \mathbf{m} is represented by the matrix \mathbf{H} composed of the elements h_{ij} . Thus,

$$\mathbf{g} = \mathbf{H}\mathbf{s} + \mathbf{n}, \quad (4)$$

where \mathbf{n} denotes the noise.

3. INFERENCE : MODELS AND ALGORITHMS

The premise for compressive sensing is that there is *a priori* knowledge about the signals of interest and the measurement provides the complementary, signal-specific information at the lowest sampling rate possible. The inference models integrate the measurement and *a priori* knowledge, which may be described in terms of physical or statistical characteristics. *A priori* knowledge is domain specific. In this manuscript, we demonstrate our inference strategies with a specific family of reflectance spectral data, described below.

The inference model may be described in general as a constrained optimization problem

$$\begin{aligned} \mathbf{s}_* &= \arg \min_{\mathbf{s}} \gamma(\mathbf{s}) \\ s.t. & \\ \mathbf{H}(\mathbf{s}) &= \mathbf{g} \end{aligned} \quad (5)$$

where the constraints are from a specific measurement model of Eqn. (4) and the objective function γ is based on a known property of the signal. With compressive sensing the null space of the sensing operator, $\text{null}(\mathbf{H})$, is multi-dimensional and there are multiple candidate solutions yielding to the same measurement \mathbf{g} . When the measurement operator is designed with respect to the *a priori* knowledge, the latter is used to distinguish the signal of choice from the other candidates.

The model is linear when the optimal solution \mathbf{s} to the problem (5) is linearly dependent on the measurement \mathbf{g} , and it is nonlinear otherwise. The algorithms for a model problem solution may be direct or iterative, depending on the model and the numerical techniques used. We describe two optimization models and the algorithms for their solutions. We evaluate the signal estimates in two aspects, one is in terms of intensity values at finer wavelength bins, the other in terms of component analysis.

The data set we use for this study is taken from the U.S. Geological Survey (USGS) Digital Spectral Library online at <http://pubs.usgs.gov/of/2003/ofr-03-395/datatable.html>. The data set consists of 500 spectra samples from natural or man-made materials such as minerals, volatiles, rocks, soils, vegetation, coatings and microorganisms as well as mathematically computed mixtures. The spectra are one dimensional signals of reflectance at given wavelengths. The database is used for remote detection of relevant materials. To simplify our test procedures, we regulate the signal to 256 equally spaced points via cubic spline interpolation. That is, each signal is composed of 256 discrete values, at equally spaced wavelengths. These spectra have previously been considered by Hamza and Brady.¹²

3.1. The least gradient model

The spectral signals of our first interest are smooth, which means that at a sufficient sampling rate, the values between the sampled values can be approximated accurately. With multiplex sensing, however, the signal is not directly sampled, although the function to be sampled is related to the signal. Based on the smoothness and the indirect measurement, we use the following least gradient (LG) model,

$$\begin{aligned} \mathbf{s}_{\text{LG}} &= \arg \min_{\mathbf{s}} \gamma(\mathbf{s}) = \|\nabla \mathbf{s}\|_2 \\ s.t. & \\ \mathbf{H} \mathbf{s} &= \mathbf{g} \end{aligned} \quad (6)$$

where ∇ denotes the discrete gradient operation. This model is linear in the sense we described earlier, although it might be mistaken as a nonlinear model from the nature of numerical procedure for the optimal solution. When discretized over equispaced samples of a signal, the gradient may be the backward difference $\nabla_k \mathbf{s} = \mathbf{s}_k - \mathbf{s}_{k-1}$, or the forward difference, or the central difference. In matrix expression, ∇ may be described as an $(n-1) \times n$ bidiagonal matrix,

$$\nabla = \begin{bmatrix} -1 & 1 & 0 & \cdots & 0 \\ 0 & -1 & 1 & \cdots & 0 \\ \vdots & \vdots & \ddots & \ddots & \vdots \\ 0 & 0 & \cdots & -1 & 1 \end{bmatrix}.$$

To get the solution to the LG model (6), we take two simple steps. First, we obtain one particular solution \mathbf{s}_p to the linear equation (4). The general solution to the equation can then be described as $\mathbf{s} = \mathbf{s}_p - \mathbf{N} \mathbf{c}$, where the columns of the matrix \mathbf{N} span the null space of \mathbf{H} , and \mathbf{c} is an arbitrary coefficient vector. The problem is reduced to a linear least squares problem without constraints,

$$\mathbf{s}_{LG} = \arg \min_{\mathbf{c}} \|\nabla(\mathbf{N} \mathbf{c} + \mathbf{s}_p)\|_2.$$

The solution to the LG problem can be expressed as follows

$$\mathbf{s}_{LG} = \mathbf{s}_p + \mathbf{N}(\mathbf{N}^T \nabla^T \nabla \mathbf{N})^{-1} (\nabla \mathbf{N})^T \nabla \mathbf{s}_p, \tag{7}$$

here we assume that the $\nabla \mathbf{N}$ is of full rank in columns. The form (7) reveals the linear relationship between the measurement and the reconstructed signal. The explicit expression of the solution suggests a simple numerical method.

The general solution (7) does not depend on the selection of a particular solution \mathbf{s}_p to the measurement equation. Some of the candidate solutions can be obtained by a direct method such as via the QR factorization of the measurement matrix, some others may require a computation procedure of iterative nature, although the computational problem is a linear one. For example, among all the candidates, there is one and only one orthogonal to the null space, *i.e.*, this particular solution has the least Euclidean length. One may get the solution of the least length via the singular value decomposition (SVD) of the measurement matrix. The SVD may be analytically available from the matrix structure or obtained numerically. The latter approach is in general an iterative process.

In Figure 3, we show a particular signal, and an estimate of the signal based on the LG model. The plot to the left show the overall agreement between the original signal and the estimate, while the plot to the right shows a detailed view. We also show in the red dash line the least-length solutions as a particular solution to the measurement equation alone. The least-length solution via SVD is much closer to the signal than many solutions via QR to the measurement equation, but it is still improved substantially by the LG optimization step.

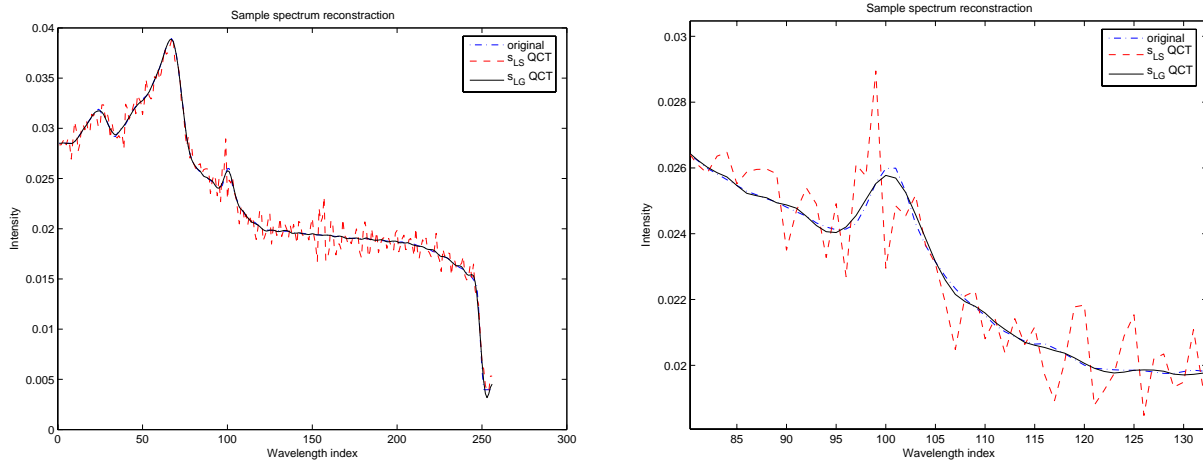


Figure 3. The original signal \mathbf{s} in blue dash-dot line, the LG estimate \mathbf{s}_{LG} in green solid line, and the least-length solution \mathbf{s}_{LS} in red dash line as a particular solution to the measurement equation, at the measurement-estimation ratio = 64 : 256. Left: the overall density distribution; Right : a zoomed-in view.

3.2. Component analysis

We give some evaluation of the signal estimates by the LG model. Rather than using the same metrics on the intensity values at the given wavelengths, we examine and evaluate the information captured by the compressive measurement and the inference from a different perspective, namely, in terms of signal components other than

wavelengths. Here we use the principle components (PC) in the statistical sense. To this end, we divide the data set into two subsets, one for gathering the statistics of the signal data (the training dataset), the other is used for evaluating the fidelity in signal estimates (the test dataset). A signal estimate is evaluated as follows. First, we examine the accuracy of each individual PC coefficient in a group of dominant principle components. The dominant components are specific to the signal, not predetermined by the training set. Second, we evaluate the relative presence in the distribution of the non-dominant PC coefficients.

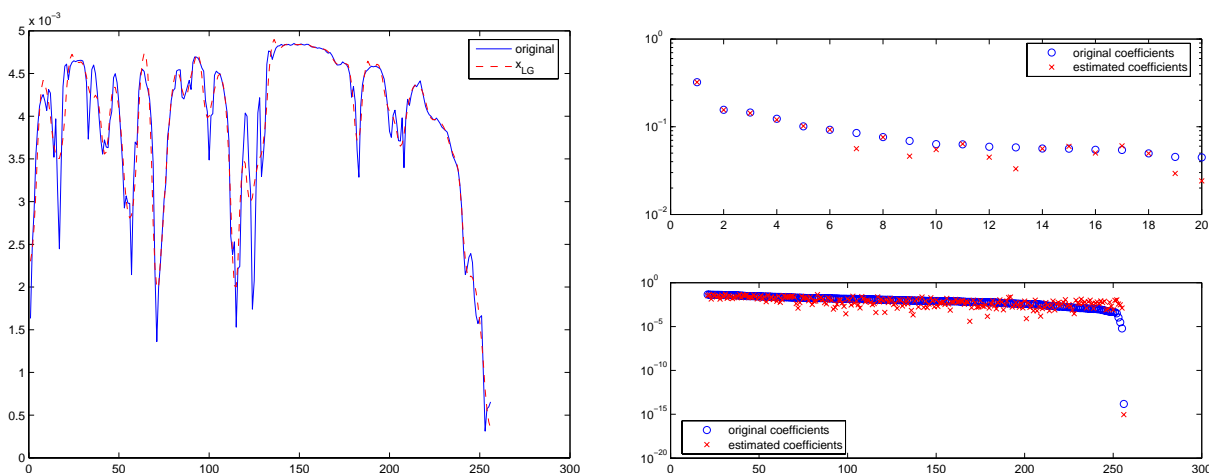


Figure 4. Left: a test signal \mathbf{s} in blue line and the LG estimate \mathbf{s}_{LG} in red line; Right: the signal-specific PC coefficients, the 20 most dominant at the top and the rest at the bottom.

In Figure 4 we show a test signal, and its estimate, in terms of its intensity values at 256 wavelengths, to the left, and its PC coefficients, to the right. Again, the measurement has only 64 values. The particular signal is perhaps the most challenging one in the test set. At the top right, we show in detail the 20 dominant PC coefficients in the test signal and the corresponding ones in the estimated signal. The signal-specific dominant PCs are $\{3, 1, 9, 8, 10, 7, 76, 11, 80, 26, 5, 29, 86, 4, 53, 12, 40, 2, 94, 67\}$ in the PCs of the training set in the descending order of the singular values. The first 6 coefficients are accurately estimated. There is slight deviation in some of the next 14 coefficients. To show the agreement and deviation clearly, the coefficients are shown in the log of their absolute values. The signs of the coefficients match. The rest of the coefficients are shown in the plot at the bottom right. The distribution of the coefficients in the signal estimate agrees with that of the source signal.

Some remarks are in order. The above worst-case analysis demonstrates that the essential PC information is captured with the compressive sensing, waiting to be revealed or enhanced by the subsequent application of inference algorithms. We had considered direct estimation of the PC coefficients from compressive sensing. The resulting estimates, even with the known location of the dominant PCs, are far from satisfactory. The coefficient distribution, as shown in Figure 4, offers the explanation. It shows that the PC coefficients in the trailing end are not negligible altogether. This means that a truncation in the PC coefficients is inadequate for this situation, including a truncation based on the assumption of the sparsity in the PC coefficients. There are situations where linear projections or truncations are well applicable for compressive sensing.¹ The reverse, however, is not necessarily true. There are arguably more circumstances where there exist additional, and most likely, nonlinear relationships between the components. A truncation between tangled components would degrade the fidelity in signal estimates. In fact, we view the unsatisfactory estimates generated by truncation schemes as an indication of an interdependent relationship between the components. For the set of data concerned in this study, there are physical reasons to expect such interdependence between components. A statistical inference model could describe the intimate relationship between the measured values and the missing or hidden values. Modeling such a statistical relationship is a subject of ongoing research in our group.

3.3. The adaptive LG model

In this section we introduce the adaptive version of the least-gradient model. The measurement is signal specific. The metric used in the objective function in the LG model of (6), however, favors smoother estimate candidates. The essentially quadratic objective function has the advantage in both convenient analysis and computation of the optimization problem. To make the LG model more adaptive while continue exploiting the advantage of the quadratic form, we adapt the metric weights, \mathbf{w} , on the signal gradient to the signal feature, instead of fixing the weights equally,

$$\arg \min_{\mathbf{s}} \|\nabla \mathbf{s}\|_{\mathbf{w}} = \|\mathbf{w} \cdot * \nabla \mathbf{s}\|_2. \quad (8)$$

The key is the determination of the adaptive weights. We have experimented with two adaptive strategies. Both the strategies use initially the least-length solution with equal weights. In the first strategy, we lower the weights at the critical points in the least-gradient solution. Here, the critical points refer to the maximum, minimum or saddle points in local regions. This strategy enhances the contrast between peaks and the transition areas between the peaks in the LG estimate. In the second strategy, the adaptive weights are determined by a scan of a small weight window over the LS estimate. We use the the local response to the change in the weights to reveal the peaks still hidden in the LG estimate. In Figure 5, we show in a zoomed-in view the effects of the adaptation strategies at a few intensity peaks. The test signal is the same as that in Figure 4, the compression rate remains at 64 : 256.

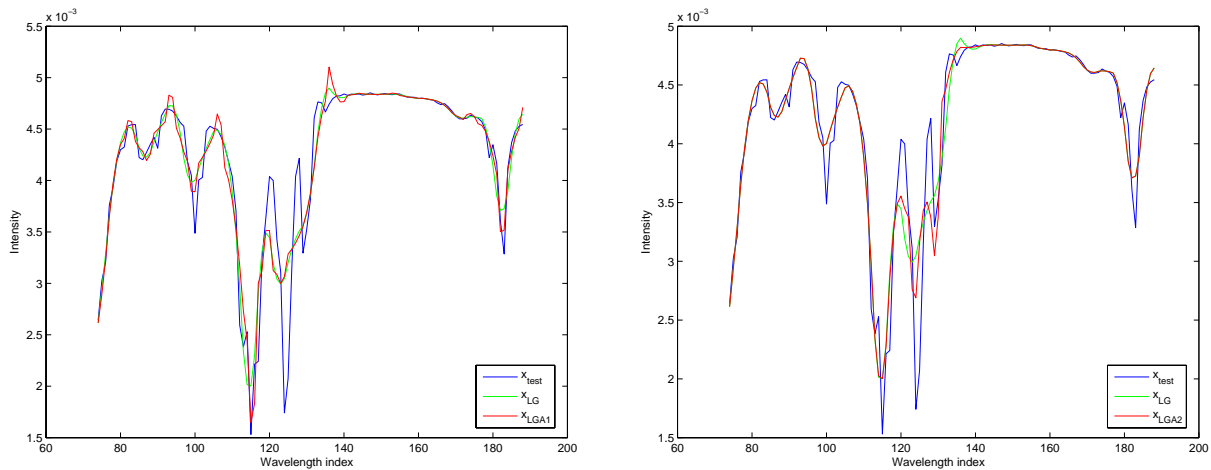


Figure 5. The test signal is in blue solid line, the LG estimate is in green line, and the adjusted estimate is in red line. Left: the enhanced estimate with the critical-point-based weighting scheme. Right: the estimate improved further by the scan-response-based weighting scheme.

Since the metrics in the objective function are changed adaptively, we use the PC analysis as the basis for quantitative evaluation of the improvement in signal estimates. The accuracy of the 5 coefficients with the dominant PCs immediately next to the leading one are all improved, and the coefficients get closer, over all, to those of the test signal. This improvement again shows that the essential information is captured by the compressive sensing, waiting to be revealed by the application of the proper inference algorithm. The adaptive version of the LG model and the adaptation techniques are very promising for high-fidelity inference. We will give an elaborate description of the adaptation process elsewhere.

4. CODESIGN PRINCIPLES

Spectrometer design for the systems described here consists of determination of \mathbf{K} and \mathbf{H} such that the solution to the constrained optimization problem

$$\begin{aligned} \mathbf{s}_{\text{LK}} &= \arg \min_{\mathbf{s}} \|\mathbf{K}(\mathbf{s})\|_2 \\ \text{s.t.} & \\ & \mathbf{H}\mathbf{s} = \mathbf{g}, \end{aligned} \quad (9)$$

is a satisfactory estimate of \mathbf{s} . The operator \mathbf{K} may describe either physical or statistical characteristics, or both. As described in Section 3.3, one may incorporate in the operator \mathbf{K} different types of metrics, nonlinearity, and adaptation. In realizable physical systems, \mathbf{H} cannot be arbitrarily specified. As reflected in Eqn. (1) and subsequent discussion, the simplest constraint is $0 \leq h_{ij} \leq 1$. Variations on spectrometer designs with different spatial coherence and sampling strategies may further constrain h_{ij} , such as $h_{ij} \in \{0, 1\}$. If compression is not an issue, one may consider measurement of principal components based on complementary positive and negative projections, but with compressive sensing as a goal this is not feasible. In addition to the problem formulation framework of (9) and the limitation in physical realization, we describe three co-design principles below.

The two operators \mathbf{H} and \mathbf{K} shall be designed so that the solution to (9) is unique. For the specific LG model (6), this condition means that the sensor-reconstruction product matrix $\nabla\mathbf{N}$ be of full rank in columns. In general, we pose the *consistency condition*: the null space of the sensing operator does not contain the constant signals. It is necessary for the uniqueness; otherwise even the constant signals are not guaranteed to be reconstructed correctly. In practice, the consistency condition can be met easily. For example, we let the row space of \mathbf{H} contain the row vector, \mathbf{e}^T , with all the elements equal to 1. Specifically, we may assume that \mathbf{e}^T is a row of \mathbf{H} . In this way, the operator is designed to make the constant vector orthogonal to the null space of \mathbf{H} ,

$$\mathbf{e}^T\mathbf{N} = 0. \quad (10)$$

This orthogonal consistency condition is necessary to ensure that the reconstruction error has zero mean. It is also sufficient for the uniqueness of solution. Suppose $\nabla\mathbf{N}\mathbf{c} = 0$ for some nonzero coefficient vector \mathbf{c} . Then,

$$\begin{pmatrix} \mathbf{e}^T \\ \nabla \end{pmatrix} \mathbf{N}\mathbf{c} = 0, \quad \mathbf{c} \neq 0.$$

On the other hand, the matrix composed of \mathbf{e}^T and ∇ is non-singular and, when multiplied to \mathbf{N} , preserves the full column-rank of \mathbf{N} . This contradiction shows that $\nabla\mathbf{N}$ is of full column rank under the condition (10). For example, when $\mathbf{K} = \nabla^2$ is the second order difference, the null space of \mathbf{K} is two dimensional, containing all linear functions. It is necessary for the row space of \mathbf{H} to contain the constant vector so that the reconstruction error has zero mean. It is sufficient for the zero-mean error condition and for the uniqueness of the solution that $\text{null}(\mathbf{H})$ and $\text{null}(\mathbf{K})$ are orthogonal.

Another design issue, especially important for compressive sensing, is to make the sensing and reconstruction models complementary to each other. For example, if the null space of \mathbf{H} is a proper invariant subspace of $\nabla^T\nabla$, then the least-gradient solution does not improve the least-length solution, because they are one and the same, by the expression of the solution in (7). With respect to the LG model, we therefore select the measurement mapping \mathbf{H} so that the rows of the matrix are not orthogonal to any invariant subspace of $\nabla^T\nabla$.

The most delicate codesign issue lies in modeling and exploiting the relationship between the measured values and the hidden values. Such coupling relationship exists in many circumstances, such as in the family of spectral data we used in this study. The existence of the coupling relationship is the premise of compressive sensing systems. The relationship is integratedly described in the inference model and encoded in the measurement model. The modeling techniques may vary in many different ways, we have described a few particular ones in this paper.

ACKNOWLEDGMENTS

This work was supported by the Defense Advanced Research Agency under grant number W911NF-04-1-0319.

REFERENCES

1. D. L. Donoho, "Compressed sensing," tech. rep., Stanford University, September 2004.
2. Y. Tsaig and D. L. Donoho, "Extensions of compressed sensing," tech. rep., Stanford University, October 2004.
3. D. J. Brady, N. P. Pitsianis, and X. Sun, "Reference structure tomography," *JOSA A* **21**(7), pp. 1140–1147, 2004.
4. N. P. Pitsianis, D. J. Brady, and X. Sun, "Sensor-layer image compression based on the quantized cosine transform," *Visual Information Processing XIV* **5817**(1), pp. 250–257, SPIE, 2005.
5. D. J. Brady, M. Feldman, N. Pitsianis, J. Guo, A. Portnoy, and M. Fiddy, "Compressive optical montage photography," *Photonic Devices and Algorithms for Computing VII* **5907**(1), p. 590708, SPIE, 2005.
6. A. D. Portnoy, N. P. Pitsianis, D. J. Brady, J. Guo, M. A. Fiddy, M. R. Feldman, and R. D. T. Kolste, "Thin digital imaging systems using focal plane coding," *Computational Imaging IV* **6065**(1), p. 60650F, SPIE, 2006.
7. P. Potuluri, *Multiplex Optical Sensors for Reference Structure Tomography and Compressive Spectroscopy*. PhD thesis, Duke University, August 2004.
8. D. Wilson and H. Barrett, "Decomposition of images and objects into measurement and null components," *Optics Express* **2**(6), pp. 254–260, 1998.
9. M. Gehm, S. McCain, N. Pitsianis, D. Brady, P. Potuluri, and M. Sullivan, "Static 2d aperture coding for multimodal multiplex spectroscopy," *Applied Optics*, p. to appear May 2006, 2006.
10. S. McCain, M. Gehm, Y. Wang, N. Pitsianis, and D. Brady, "Coded aperture raman spectroscopy for quantitative measurements of ethanol in a tissue phantom solution," *Applied Spectroscopy*, p. to appear, 2006.
11. P. Potuluri, M. E. Gehm, M. E. Sullivan, and D. J. Brady, "Measurement-efficient optical wavemeters," *Optics Express* **12**, pp. 6219–6229, 2004.
12. A. B. Hamza and D. J. Brady, "Reconstruction of reflectance spectra using robust non-negative matrix factorization," to appear in *IEEE Transactions on Signal Processing*.